



# Dissection and validation of a promising QTL controlling spikelet number on 5B in bread wheat

Yaoqi Si<sup>1</sup> · Shuiquan Tian<sup>1,2</sup> · Jianqing Niu<sup>1</sup> · Zhongqing Yu<sup>3</sup> · Shengwei Ma<sup>1</sup> · Qiao Lu<sup>2</sup> · Huilan Wu<sup>1,2</sup> · Hong-Qing Ling<sup>1,2</sup> · Shusong Zheng<sup>1,2</sup>

Received: 2 June 2023 / Accepted: 16 October 2023 / Published online: 6 November 2023  
© The Author(s), under exclusive licence to Springer-Verlag GmbH Germany, part of Springer Nature 2023

## Abstract

**Key message** Five environmentally stable QTLs for spikelet number per spike and days to heading were identified using a high-genetic map containing 95,444 SNPs, among which *Q<sub>Sns.ucas-5B</sub>* was validated using residual heterozygous line at multiple environments.

**Abstract** Spikelet number per spike (SNS) and days to heading (DTH) play pivotal roles in the improvement of wheat yield. In this study, a high-density genetic map for a recombinant inbred lines (RILs) population derived from Zhengnong 17 (ZN17) and Yangbaimai (YBM) was constructed using 95,444 single-nucleotide polymorphism (SNP) markers from the Wheat660K SNP array. Our study identified a total of five environmentally stable QTLs for SNS and DTH, one of which was named *Q<sub>Sns.ucas-5B</sub>*, with a physical interval of approximately 545.4–552.1 Mb on the 5BL chromosome arm. Importantly, the elite haplotype within *Q<sub>Sns.ucas-5B</sub>* showed a consistent and positive effect on SNS, grain number and weight per spike, without extending the days to heading. These findings provide a foundation for future efforts to map and clone the gene(s) responsible for *Q<sub>Sns.ucas-5B</sub>* and further indicate the potential application of the developed and validated InDel marker of *Q<sub>Sns.ucas-5B</sub>* for molecular breeding purposes, aimed at improving wheat grain yield.

## Introduction

Wheat is one of the major grain crops in the world and provides approximately 20% of the calories in the human diet (Simmonds et al. 2016). The reduction in arable land area, climate change and the rapid increase of global population have created an urgent need for breeders to breed high-yield wheat varieties to secure global wheat production. Wheat

yield can be largely partitioned into three components, including spike number per hectare, grain number per spike (GNS) and thousand kernel weight (TKW) (Isham et al. 2021). Generally, GNS can be further subdivided into spikelet number per spike (SNS) and grains per spikelet (Quarrie et al. 2006). Numerous reports have demonstrated that an increased SNS could increase the yield potential of wheat (Chen et al. 2022; Zhang et al. 2022). Thereby, modifying SNS could be a strategy for improving yield potential of wheat as it is associated with higher GNS (Lewis et al. 2008; Wang et al. 2022).

SNS is a complex quantitative trait controlled by multiple genes as well as environmental factors (Corsi et al. 2021; Muqaddasi et al. 2019). The application of molecular markers associated with SNS would increase the efficiency for improving yield potential attained via modern wheat breeding, such as marker-assisted selection (MAS) (Chhetri et al. 2017; Wurschum et al. 2018). Thus, determination of the chromosomal localization, number and genetic effects of the corresponding genes is desirable for obtaining optimal genotype in wheat breeding. However, due to the complexity of wheat genome and the compensatory effects of homoeologous genes, only a few genes involved in spike morphology

Yaoqi Si, Shuiquan Tian and Jianqing Niu have equally contributed to this work.

✉ Hong-Qing Ling  
hqling@genetics.ac.cn

✉ Shusong Zheng  
shusong@genetics.ac.cn

<sup>1</sup> State Key Laboratory of Plant Cell and Chromosome Engineering, Institute of Genetics and Developmental Biology, The Innovative Academy of Seed Design, Chinese Academy of Sciences, Beijing 100101, China

<sup>2</sup> College of Advanced Agricultural Sciences, University of Chinese Academy of Sciences, Beijing 100049, China

<sup>3</sup> National Key Laboratory of Crop Biology, College of Life Sciences, Shandong Agricultural University, Taian, China

or SNS have been characterized through homologous cloning method or map-based cloning (Huang et al. 2009; Zhang et al. 2015). For example, the photoperiod-sensitive gene *Photoperiod1* (*Ppd1*), the wheat *FRIZZY PANICLE* (*WFZP*) gene, the well-known maize (*Zea mays* L.) domestication gene *TEOSINTE BRANCHED1*, and *DUO-B1* (*DUO* means more in Chinese) have been found to regulate the formation of “paired spikelet” (the supernumerary spikelet) in wheat (Boden et al. 2015; Dixon et al. 2018; Dobrovolskaya et al. 2015; Li et al. 2021b; Wang et al. 2022). In addition, the domestication gene *Q*, which encodes a member of AP2 transcription factor family, not only affects threshability and spike architecture, but also changes flowering time and plant height (He et al. 2021; Liu et al. 2020; Simons et al. 2006; Song et al. 2019; Zhao et al. 2018). The transgenic wheat plants carrying extra copies of *WAP0-A1* driven by its native promoter had more spikelet, a more compact spike apical region and smaller terminal spikelet than the wild type (Kuzay et al. 2022). Constitutive overexpression of the dominant *TaCol-B5* allele (without the region encoding B-boxes), a rare allele in a global collection of modern wheat cultivars, in the common wheat cultivar Yangmai 18 increased SNS as well as tillers and spikes, thereby enhancing grain yield averaging an 11.9% compared to wild-type under field conditions (Zhang et al. 2022).

An increasing body of evidence suggests that genes belonging to the heading date pathway exert influence on spikelet differentiation and maximum spikelet number per spike (Sreenivasulu and Schnurbusch 2012). Notably, *Ppd1* has been shown to prolong the period of floral initiation, delaying heading date and increasing the spike length and number of spikelets per spike (Okada et al. 2019). Furthermore, null mutants of *FLOWERING LOCUS T2* (*FT2*) and *FT-D1* have been observed to display increased maximum spikelet number per spike, accompanied by a prolonged period of spike development in common wheat (Chen et al. 2022; Shaw et al. 2018).

QTL mapping is a traditional genetic tool for dissecting genetic basis of key traits related to grain yield. It provides molecular markers closely related to yield component traits and increased the genetic gains in breeding process by MAS. Numerous QTLs for SNS have been identified on almost all the 21 chromosomes in wheat by bi-parental QTL mapping or genome-wide association studies (GWAS) (Cui et al. 2012; Echeverry-Solarte et al. 2015; Li et al. 2021a; Xu et al. 2022; Yao et al. 2019). For example, Ma et al. (2007) reported a QTL (*QSpn.nau-5A*) for SNS on 5A chromosome using RIL and immortalized  $F_2$  populations, which simultaneously affected spike length and spike density. Xu et al. (2022) identified two QTLs (*QTsn.cau-5D.3* and *QTsn.cau-6D*) for SNS derived from the D genome of the natural and resynthetic allohexaploid wheat. Furthermore, with the advent of high-density genotyping assays, such as

the wheat 55 K (Liu et al. 2018), 90 K (Chen et al. 2020) and 660 K (Cui et al. 2017; Sun et al. 2020) SNP arrays, significant progress has been reported for QTL associated with yield component traits. For example, Sun et al. (2017) revealed new allelic variation distribution for SNS by GWAS method with the wheat 90K assay and found 116 significant SNPs were associated with SNS; the phenotypic variation explained (PVE) by each SNP ranged from 15.5 to 33.7%. Chen et al. (2020) found a QTL for SNS on the short arm of chromosome 7A, which had the pleiotropic effects of *FT-A1*, a gene controlling flowering time. Li et al. (2021a) identified a novel QTL *QTsn/Fsn.cib-3D* associated with both SNS and fertile spikelet number per spike located in a 4.5-cM interval on chromosome arm 3DL. Nevertheless, only a few of QTLs have been genetically verified, which greatly restrict the dissection of the molecular basis underlying spikelet number. Thus, the identification and verification of novel QTL/genes for SNS are desirable for obtaining optimal genotype during breeding practices.

In this study, we constructed a RIL population derived from a cross between two winter wheat varieties, built a high-density genetic map with SNPs from the Wheat660K SNP array, evaluated SNS and DTH of this population in multiple environments, explored the QTL for SNS and DTH and identified a promising QTL on chromosome 5BL. We further validated the QTL by residual heterogeneous line (RHL) in the field trials. Collectively, these data provide further insight for the genetic basis of spikelet development in wheat, and the related linkage marker will be useful for marker-assisted selection in wheat improvement.

## Materials and methods

### Mapping populations

QTL mapping was performed using a  $F_8$  RIL population with 188 lines derived from a cross between the winter common wheat lines Zhengnong17 (ZN17) and Yangbaimai (YBM) (denoted as ZY-RILs) by the single seed descent method described by Si et al. (2021). ZN17 is an elite parent carrying the 1BL.1RS translocation, while YBM is a Chinese landrace characterized by high tiller number. For phenotyping, the ZY-RILs population along with two parents were planted at the following two experimental locations: Zhaoxian county, Hebei province (37° 50' N, 114° 49' E) and Beijing (40° 16' N, 116° 24' E), China. The field trials were carried out in four growth seasons (2016–17, 2017–18, 2018–19 and 2020–21) at Zhaoxian with multiple fertilizer treatments, and one crop season (2016–17) at Beijing. The detailed information of nine trials was described in Supplementary Table S1 (referred to as E1–9). These field trials were arranged in an alpha-lattice block design with

two replications, and each plot consisted of two one-meter-long rows with the row-space of 25 cm. All trials were sown by hand with the aid of a homemade hole digger, which punched 11 seeding holes with 10 cm space between adjacent holes each time.

A RHL (RIL-55,  $F_9$ ) was identified from ZY-RILs population using a QTL-specific marker *InDel-SNS5B* and self-pollinated to produce two homogeneous lines RHL-55<sup>ZN17</sup> (genotype same with ZN17) and RHL-55<sup>YBM</sup> (genotype same with YBM) with contrasting alleles at *QSn.sucas-5B* region. Additionally, a secondary segregating population derived from RIL-55 was employed for the confirmation of the effect of *QSn.sucas-5B*. The RHL-55<sup>ZN17</sup> and RHL-55<sup>YBM</sup> pairs were genotyped to identify the consistency of genetic background using the wheat660K SNP array. The RHL-55<sup>ZN17</sup> and RHL-55<sup>YBM</sup> pairs were sown in four environments to evaluate the genetic effect of *QSn.sucas-5B* at Zhaoxian county (E6–8) and Beijing (2018BJ) during the 2018–19 wheat growing seasons.

### Phenotype evaluations and statistical analyses

The DTH of each RIL was computed as the number of days elapsed from the day of sowing to the date when roughly 50% of spikes became visible. The SNS values were determined as the average SNS from ten randomly selected main spikes in the middle region of each plot right before harvest. For each genotype, the average values of SNS across all replicates were used to represent the data in each environment. Lastly, the DTH was investigated in a total of seven environments (E2–8), while the SNS was examined in nine environments (E1–9). The best linear unbiased predictions (BLUP) values for each trait were calculated using the ANOVA function in IciMapping v4.2 (<https://isbreeding.caas.cn/>) (Meng et al. 2015), and the corresponding normal distribution was tested by the Shapiro–Wilk test ( $p=0.05$ ) with IBM SPSS Statistics 19 (SPSS, Chicago, USA). The broad-sense heritability ( $H_B^2$ ) for SNS and DTH were calculated following the formula  $H_B^2 = \sigma_g^2 / (\sigma_g^2 + \sigma_{ge}^2/n + \sigma^2/nr)$ , where  $\sigma_g^2$  denotes the genotypic effect,  $\sigma_{ge}^2$  represents the genotype by environmental effect,  $\sigma^2$  signifies the residual error,  $n$  stands for the number of environments, and  $r$  is the number of replicates (Holland et al. 2003).

### Genetic map construction and QTL detection

The ZY-RILs population and their parents were genotyped using the wheat660K Illumina iSelect array in the company of CapitalBio Technology (Beijing) as described in Si et al. (2021). The SNP was remained if it pass all of the following criterions: (1) Polymorphic between the two parents; (2) Missing rate < 5% (the heterozygous SNP was regarded as

missing); (3) Unique mapped against the reference genome of IWGSC RefSeq v2.1 (Zhu et al. 2021). Redundant SNP markers were removed using the “BIN” function of IciMapping v4.2 as described by Li et al. (2021a), and only bin markers containing at least two SNP markers were retained (Ronin et al. 2017). Specifically, the best marker (with the lowest missing rate) for each BIN marker was selected for the genetic map construction. Then, the BIN markers were sorted into groups and ordered using the “MAP” tool with the Kosambi mapping function of IciMapping v4.2. The parameters of “logarithm of the odds (LOD)” and “recombination fraction” were set as 3.5 and 0.3, respectively. The physical locations and chromosomal arms of the genetic maps were determined based on the blast results of the flanking sequences of BIN markers on the IWGSC RefSeq v2.1 genome assembly. The genetic maps were visualized by R package “LinkageMapView” (<https://github.com/louellette/LinkageMapView>).

The observed phenotypic values of each trait obtained from each environment were used for QTL detection using the inclusive composite interval mapping (ICIM) method by the software IciMapping v4.2. In QTL analysis, the missing phenotype was deleted and the walking speed was 1.00 cM, with a  $p$  value inclusion threshold of 0.001. Furthermore, a LOD score of 3.5 was selected as a minimum to determine the presence of a QTL in a genomic region. Only QTL identified in at least three individual environments was defined as stable QTL, and these with mean PVE  $\geq 10\%$  were defined as major QTL. All QTLs were named as suggested by McIntosh et al. (2017).

### DNA extraction, gene cloning and analysis of candidate genes

High-quality DNA was extracted from young leaves of each wheat accession using the cetyl trimethyl ammonium bromide method. Genomic DNA from ZN17 and YBM was subjected to whole-genome resequencing using the DNBSEQ™ sequencer, aiming to achieve approximately 10× coverage of clean data. Subsequent to sequencing, reads obtained from these samples were aligned to RefSeq v2.1 employing the bwa software (<https://sourceforge.net/projects/bio-bwa/files/>) with default parameter configurations. SNPs and InDels situated within the genomic interval spanning from 545.4 to 552.1 Mb on chromosome 5B were identified through utilization of the HaplotypeCaller module.

For the validation of the QTL *QSn.sucas-5B*, an InDel marker *InDel-SNS5B* (F:5'GGGTCCCAAATTGTATGT CG and R:5'ACAAAGATGGAGGTCGGTGT) was designed based on the sequence variations in the target region between ZN17 and YBM. *InDel-SNS5B* was able to amplify alleles from both ZN17 and YBM, yielding products of sizes 227 and 129 bp, respectively. The

sequence of each putative candidate gene, encompassing intron, exon, 3'-UTR regions, as well as a 1-kb segment upstream of the translation initiation codon, was employed as a query for computational analysis. The design and subsequent detection of specific primers were conducted following the established protocol outlined by Si et al. (2022).

**Note** For the sake of facilitating comparison with prior research results, all coordinates involved in the manuscript were based on the IWGSC RefSeq v2.1 genome assembly.

## Results

### Linkage map construction

We used the Wheat660K SNP array to genotype the ZY-RILs population and parental lines, resulting in 630,517 SNPs, 108,987 high-quality SNPs were retained for map construction. These SNPs were grouped into 6454 bin markers, whereby bin markers containing a minimum of two SNP markers were included in the subsequent analysis. Ultimately, a sum of 2703 bin markers were successfully mapped onto the genetic map. The integrated genetic information of bins resulted in constructing a high-density map with 95,444 SNP markers spanning 4232.42 cM (Fig. 1, Supplementary Table S2). The majority of mapped SNPs were assigned to the A (53.92%) and B (38.79%) genomes, with a much lower proportion (7.29%) located on the D genome, spanning 1637.20, 1182.82 and 1412.39 cM, respectively (Table 1). Chromosome 7B had the least mapped SNP markers (268), while 5B had the most SNP markers (11,459), averaging 4544.95 loci per chromosome. Correspondingly, 7B and 5B have the least (22) and most (264) bin markers, respectively (Table 1). The average interval distance between adjacent bin markers ranges from 0.98 cM for 5B to 4.28 cM for 5D, with an average distance 1.57 cM per bin. In this study, about 5.76% of genetic gaps (the interval distance between bin markers) were more than 5 cM, and 20 gaps present in chromosomes 1D, 2A, 2D, 3A, 3B, 3D, 4A, 4D, 5D, 6A, 6B, 6D and 7D were more than 20.0 cM but less than 75.0 cM (Supplementary Table S2).

The constructed genetic map showed relatively consistent marker order with the wheat genome assembly on most chromosomes, except for part of chromosome 1A and 6B (Fig. S1). In addition, due to the 1BL/1RS translocation of ZN17, the 1RS- or 1BS-specific markers not only showed co-segregation but also exhibited distorted segregation in the ZY-RILs, resulting in only 1BL being retained. For

similar reasons, 7BS is also not shown in the constructed genetic map (Fig. S1, Supplementary Table S3).

### Phenotypic performance

Descriptive statistics of the two parental and ZY-RILs population for SNS and DTH were listed in Table 2. ZN17 exhibited a larger spikelet number and an earlier heading compared to YBM. For the ZY-RILs population, a wide and significant variation for SNS was observed, ranging from 11.9 to 27.5, whereas the differences in DTH among individuals were small (Table 2). The frequency distribution and Shapiro–Wilk test revealed that both SNS and DTH values followed an approximately normal distribution (Fig. S2), as indicated by the BLUP values. Furthermore, strong positive correlations between SNS, between DTH and between SNS and DTH values across all environments were observed (Supplementary Table S4), implying a high broad-sense heritability of SNS and DTH, and significant genetic contribution to SNS by DTH in the population.

### QTL for SNS

In the study, phenotypic data of SNS evaluated in nine environments were used for QTL mapping by IciMapping v4.2. A total of 15 QTLs for SNS were detected, which were located on chromosomes 1B, 2A, 2D, 3A, 3D, 5B, 6B and 7D, respectively. Among them, four stable environmental QTLs (*Q<sub>Sns.ucas-1B</sub>*, *Q<sub>Sns.ucas-2D.1</sub>*, *Q<sub>Sns.ucas-3D</sub>* and *Q<sub>Sns.ucas-5B</sub>*) were identified in at least five environments, explaining the phenotypic variance ranging from 1.46 to 27.96% (Table 3).

Of them, *Q<sub>Sns.ucas-1B</sub>* was detected on the end of 1B in six of nine environments, explaining 1.90–15.67% of the phenotypic variance with LOD values ranging from 4.05 to 11.72 (Table 3). *Q<sub>Sns.ucas-1B</sub>* was mapped at the beginning region of 1B flanked by SNP marker *AX-109320638* and *AX-111004440* (Fig. S3a) and physically located between 491.0 and 587.0 Mb on chromosome 1BL. Since the parent ZN17 is a 1BL.1RS translocation line and only the genetic map of 1BL was constructed in this study (Fig. S1), we speculated that the *Q<sub>Sns.ucas-1B</sub>* is likely to be located on the 1BS/1RS chromosome arm/fragment. Therefore, we selected 51 polymorphic SNPs uniformly distributed in the first 520 Mb interval of chromosome 1B and reconstructed the full-length genetic map of 1B combining with the existing 116 bin markers. The result showed that these 51 SNPs were clustered together in the genetic map, and the genetic distance between them and the nearest bin marker was more than 70 cM (Supplementary Table S5). Then, the reconstructed 1B full-length genetic map was used to map SNS again, and the result indicated that a stable QTL was located



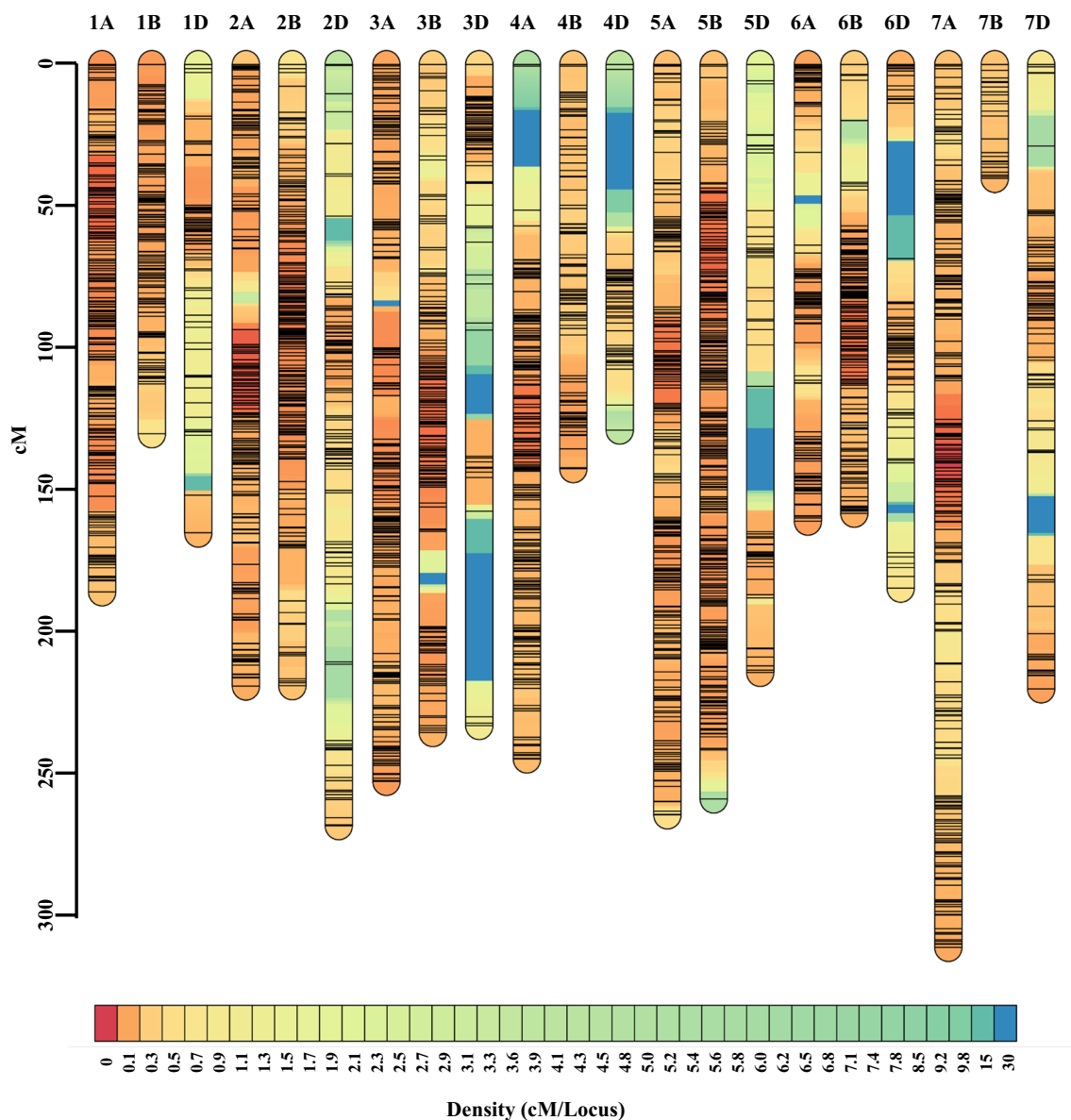


**Fig. 1** The genetic density map for the RIL population derived from ZN17 and YBM. The black bars/lines on individual chromosomes represent SNP markers. The genetic maps were visualized by R package “LinkageMapView”

on the upstream region (1BS) of the *QSns.ucas-1B* interval (Fig. S3b) and the increasing allele was derived by ZN17.

The major stable QTL on 2D, *QSns.ucas-2D.1*, was repeatedly identified in seven environments, which had LOD score of 7.46–16.95 and explained the largest phenotypic variance (5.49–23.81%) for SNS (Table 3). Remarkably, the peak marker of *QSns.ucas-2D.1* was mapped in the flanking region of *Ppd1*, a well-known gene significantly affecting spikelet number, spike length and heading date in wheat (Okada et al. 2019). As expected, the positive allele of *QSns.ucas-2D.1* was contributed by YBM. Another stable QTL was observed on chromosome 3D (*QSns.ucas-3D*) with average phenotypic variations of as much as 6.77% and YBM

contributed the increasing allele (Table 3). *QSns.ucas-5B* was significant in five environments evaluated and elucidating 3.46–8.69% of the total phenotypic variance. The allele for increased SNS in *QSns.ucas-5B* was provided by ZN17. In addition, the remaining 11 were putative QTL detected in less than three environments, explaining 3.57–22.83% of the phenotypic variation (Supplementary Table S6).

### QTL for DTH

A total of 6 QTLs associated with DTH were identified and mapped onto chromosomes 1B, 2A, 2B and 2D (Supplementary Table S6). Among them, only one stable environmental

**Table 1** General information of the high-density genetic map

| Chromosome ID | Number of SNP markers | Number of bin markers | Length (cM) | Density (cM/bin) |
|---------------|-----------------------|-----------------------|-------------|------------------|
| 1A            | 10,950                | 181                   | 185.61      | 1.03             |
| 1B            | 2387                  | 116                   | 130.02      | 1.12             |
| 1D            | 1553                  | 64                    | 164.87      | 2.58             |
| 2A            | 10,113                | 175                   | 218.81      | 1.25             |
| 2B            | 7332                  | 191                   | 218.65      | 1.14             |
| 2D            | 1003                  | 100                   | 267.99      | 2.68             |
| 3A            | 6445                  | 197                   | 252.40      | 1.28             |
| 3B            | 8369                  | 153                   | 235.22      | 1.54             |
| 3D            | 906                   | 66                    | 232.72      | 3.53             |
| 4A            | 5379                  | 184                   | 244.53      | 1.33             |
| 4B            | 1456                  | 86                    | 142.27      | 1.65             |
| 4D            | 247                   | 46                    | 128.68      | 2.80             |
| 5A            | 6475                  | 200                   | 264.24      | 1.32             |
| 5B            | 11,459                | 264                   | 258.63      | 0.98             |
| 5D            | 897                   | 50                    | 213.99      | 4.28             |
| 6A            | 2466                  | 98                    | 160.76      | 1.64             |
| 6B            | 5751                  | 141                   | 157.96      | 1.12             |
| 6D            | 748                   | 66                    | 184.32      | 2.79             |
| 7A            | 9636                  | 222                   | 310.84      | 1.40             |
| 7B            | 268                   | 22                    | 40.07       | 1.82             |
| 7D            | 1604                  | 81                    | 219.82      | 2.71             |
| A genome      | 51,464                | 1257                  | 1637.20     | 1.30             |
| B genome      | 37,022                | 973                   | 1182.82     | 1.22             |
| D genome      | 6958                  | 473                   | 1412.39     | 2.99             |
| Total         | 95,444                | 2703                  | 4232.42     | 1.57             |

QTL, designated as *QDth.ucas-2D.1* (Table 3), was identified, which showed effects across all seven environments, had a LOD value of 4.18–14.22 and delayed DTH by 0.5–1.94 days with an average of 1.45 days. This QTL explained 11.59–27.96% of the phenotypic variation. YBM conferred the effect for delaying DTH at the *QDth.ucas-2D.1* locus.

### Verification of *QSns.ucas-5B*

The residual heterozygous line provides an effective method for QTL verification without extensive backcross (Zhai et al. 2018). Based on the initial mapping result, we designed relevant detection markers and screened the ZY-RILs population for RHLs. Ultimately, a RHL (RIL-55) was selected from the ZY-RILs population with *InDel-SNS5B*, because it carried residual heterozygosity across the mapping interval of *QSns.ucas-5B*. Heterozygous  $F_2$  individuals from RIL-55 were identified and self-pollinated to produce two different homozygous genotypic lines (RHL-55<sup>ZN17</sup> and RHL-55<sup>YBM</sup>). To evaluate the

independently genetic effect of *QSns.ucas-5B*, RHL-55<sup>ZN17</sup> and RHL-55<sup>YBM</sup> were genotyped to identify the consistency of genetic background using the wheat660K SNP array. The results showed that the similarity between them was 99.73%, and only 1,153 SNPs were different (Fig. 2a). Of these polymorphic SNPs, 523 (45.36%) were located on chromosome 5B, mainly (457, 91.6%) spanning the physical intervals 545.4–559.5 Mb in the IWGSC RefSeq v2.1 sequence (Fig. 2b). To further validate and investigate the effect of *QSns.ucas-5B* for SNS, the RHL-55<sup>ZN17</sup> and RHL-55<sup>YBM</sup> pairs were evaluated in four field trials. Compared with RHL-55<sup>YBM</sup>, RHL-55<sup>ZN17</sup> showed a significant increase in SNS ranging from 1.31 (6.74%) to 2.54 (13.17%) (Fig. 2c). In addition, a secondary segregating population derived from the residual heterozygous line (RIL-55) at the *QSns.ucas-5B* locus was analyzed, revealing that the materials carrying the ZN17 haplotype (RHL-ZN17) at this locus had significantly higher SNS compared to the materials carrying the YBM haplotype (RHL-YBM) (Fig. 2d). Collectively, these results demonstrated that the ZN17 haplotype in *QSns.ucas-5B* has a consistent positive effect on SNS, and *QSns.ucas-5B* are likely to be located within the physical interval of approximately 545.4–552.1 Mb on chromosome 5B.

Additionally, we further analyzed the effects of *QSns.ucas-5B* on other yield-related traits including plant height (PH), spike number (SN), seed length (SL), seed width (SW), grain weigh per spike (GWS), TKW, GNS and DTH in the ZY-RILs populations based on the genotype detected by marker *InDel-SNS5B*. The result showed that the positive alleles contributed by ZN17 were identified with a significant influence on SNS, GNS and GWS in ZY-RILs population (Fig. 3a–c), while the differences for PH, SN, SW, SL and TKW between the two alleles were not significant (Fig. 3d–h). In addition to the increase in spikelet number, the identified locus *QSns.ucas-5B* was found to significantly reduce the days to heading (Fig. 3i). A congruent observation is that RHL-55<sup>ZN17</sup> exhibited a significant reduction in the days to heading as compared to RHL-55<sup>YBM</sup> (Fig. S4). These results indicate that the developed InDel marker in conjunction with *QSns.ucas-5B* has potential applications in wheat breeding.

### Candidate genes for *QSns.ucas-5B*

There were 63 high-confidence genes within the interval of *QSns.ucas-5B* (545.4–552.1 Mb of the IWGSC RefSeq v2.1 sequence, Supplementary Table S7). To further identify possible candidate genes in the candidate region, we resequenced both parents. Resequencing analysis of ZN17 and YBM revealed the presence of 22,354 SNPs/InDels variations within the candidate region (Supplementary Table S8). Additionally, an analysis of differential SNPs/

**Table 2** Phenotypic variation and heritability of SNS and DTH for the parents and the ZY-RILs population in different environments

| Trait | Environment | Parents  |          | The ZY-RILs population |             | $H^2$ |
|-------|-------------|----------|----------|------------------------|-------------|-------|
|       |             | ZN17     | YBM      | Mean                   | Range       |       |
| SNS   | E1          | 21.2±1.6 | 20.0±1.2 | 21.5                   | 17.2–25.4   | 0.95  |
|       | E2          | 21.1±1.3 | 20.1±1.0 | 21.4                   | 16.9–25.2   |       |
|       | E3          | 16.8±1.0 | 15.8±0.5 | 19.1                   | 14.0–24.9   |       |
|       | E4          | 19.0±1.0 | 16.4±1.4 | 18.2                   | 15.2–21.6   |       |
|       | E5          | 18.2±1.2 | 17.1±1.1 | 16.5                   | 11.9–20.6   |       |
|       | E6          | 20.1±1.0 | 19.3±0.7 | 21.0                   | 15.8–27.5   |       |
|       | E7          | 19.8±1.1 | 18.9±0.7 | 20.5                   | 16.2–25.1   |       |
|       | E8          | 20.1±2.1 | 17.3±0.9 | 19.7                   | 16.2–24.9   |       |
|       | E9          | 22.0±0.6 | 20.4±1.0 | 22.0                   | 17.4–27.2   |       |
| DTH   | E2          | 200      | 203      | 199.1                  | 197.0–205.0 | 0.91  |
|       | E3          | 201      | 204      | 203.4                  | 198.3–215.5 |       |
|       | E4          | 197      | 199      | 200.3                  | 196.0–212.3 |       |
|       | E5          | 198      | 200      | 200.3                  | 196.0–209.0 |       |
|       | E6          | 202      | 205      | 205.2                  | 199.5–213.0 |       |
|       | E7          | 202      | 202      | 203.1                  | 195.0–210.0 |       |
|       | E8          | 198      | 199      | 201.0                  | 193.0–207.5 |       |

SNS spikelet number per spike, DTH days to heading.  $H^2$  broad-sense heritability

InDels revealed amino acid differences between the parents in 15 genes (Supplementary Table S9). In rice, the B3 domain proteins play important roles in the development of rice heading and panicle architecture (Peng et al. 2007; Song et al. 2018). Interestingly, among the 15 polymorphic proteins identified between the parental lines, *TraesCS5B03G0915200* encodes a B3 domain-containing protein and exhibits pronounced expression levels in the spike tissue (Fig. S5), which may be the candidate gene. DNA sequence analysis showed that there were 2 SNPs and 2 InDels between *TraesCS5B03G0915200* of parental lines ZN17 and YBM, including 1 SNPs and 1 InDel in exon, 1 InDels in 3'-UTR region and 1 SNP in intron (Fig. S6). Furthermore, we have identified that *TraesCS5B03G0911400* encodes a guanine nucleotide exchange family protein, which exhibits high expression in the spike (Fig. S5). The homologous gene mutation of *TraesCS5B03G0911400* in rice have been found to impact lateral root development (Kitomi et al. 2008), which may have implications for nutrient and water uptake, resulting in hindered plant growth and development. Sequencing results indicate a single-base deletion (C) at position 3523 in YBM compared to ZN17, resulting in a frameshift mutation in the gene. Taken together, our findings suggest that *TraesCS5B03G0915200* and *TraesCS5B03G0911400* may exert a regulatory role in determining SNS.

## Discussion

Spikelet number per spike and heading date are critical traits affecting wheat yield improvement. In the current research, we assessed the QTL for SNS and DTH in a recombinant inbred line population across multiple environments. Our results identified and validated a stable QTL, *Qsns.ucas-5B*, which was significantly associated with grain number per spike and grain weight per spike. Importantly, this QTL does not lead to delayed heading in wheat, which adds further value to its significance for genetic improvement of wheat yield.

### Comparison of constructed genetic linkage maps with previous reports

QTL analysis is an effective and widely used strategy in the genetic dissection of complex traits in wheat, and high-density genetic maps play a crucial role in the accuracy of QTL mapping. In the present study, we constructed a high-density genetic map containing 95,444 SNPs with a total length of 4232.42 cM using the wheat660 SNP array (Fig. 1, Table 1). Compared with another genetic map constructed with SNPs of the wheat660K array, which included 119,566 markers, 4959 bin markers and a total length of 4424.4 cM (Cui et al. 2017), the genetic map constructed in this study contains fewer SNP and bin (2703) markers, while with similar genetic distance (Table 1). The average genetic distance per bin marker in this study (1.57 cM) was greater than that of Cui et al. 2017 (0.9 cM), possibly due to the deletion of all bin markers without co-isolated SNP markers. The genetic

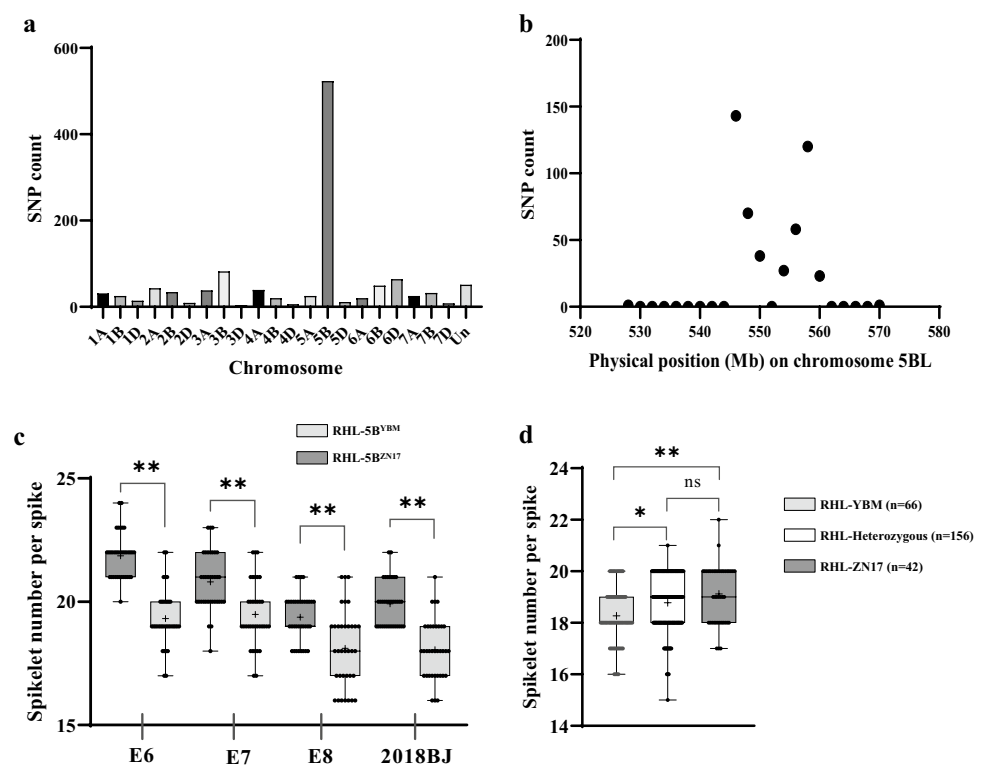
**Table 3** Summary of environmentally stable QTLs detected in the ZY-RILs population

| Trait                          | QTL                              | Env. | Pos. (cM) | Interval (cM) | Left marker  | Right marker | LOD   | PVE (%) | Add   | Physical Pos. (Mb) | References and known gene <sup>a</sup>                                 |
|--------------------------------|----------------------------------|------|-----------|---------------|--------------|--------------|-------|---------|-------|--------------------|--|
| SNS                            | <i>Q<sub>Sns.ucas-1B</sub></i>   | E1   | 0         | 0–2.5         | AX-109320638 | AX-111004440 | 11.72 | 15.67   | -0.47 | 491.0–587.0        | Ma et al. (2019), Okada et al. (2019), Zhou et al. (2017); <i>ppd1</i> |
|                                |                                  | E5   | 0         | 0–5.5         | AX-109320638 | AX-111004440 | 7.65  | 8.48    | -0.42 | 491.0–587.0        |  |
|                                |                                  | E6   | 0         | 0–6.5         | AX-109320638 | AX-111004440 | 7.43  | 11.27   | -0.62 | 491.0–587.0        |  |
|                                |                                  | E2   | 0         | 0–6.5         | AX-109320638 | AX-111004440 | 5.52  | 1.90    | -0.36 | 491.0–587.0        |  |
|                                |                                  | E7   | 0         | 0–8.5         | AX-109320638 | AX-111004440 | 4.20  | 8.24    | -0.40 | 491.0–587.0        |  |
|                                |                                  | E4   | 2         | 0–9.5         | AX-109320638 | AX-111004440 | 4.05  | 6.95    | -0.37 | 491.0–587.0        |  |
|                                |                                  | E2   | 54        | 48.5–57.5     | AX-110586525 | AX-110595669 | 12.02 | 5.49    | 0.59  | 18.6–30.1          |  |
|                                |                                  | E1   | 57        | 52.5–57.5     | AX-110595669 | AX-110006357 | 7.46  | 9.51    | 0.36  | 30.1–30.8          |  |
|                                |                                  | E6   | 58        | 56.5–65.5     | AX-110006357 | AX-109421639 | 10.21 | 16.37   | 0.73  | 30.8–52.0          |  |
|                                |                                  | E9   | 58        | 56.5–61.5     | AX-110006357 | AX-109421639 | 14.83 | 23.29   | 0.74  | 30.8–52.0          |  |
| <i>Q<sub>Sns.ucas-3D</sub></i> | <i>Q<sub>Sns.ucas-3D</sub></i>   | E5   | 60        | 57.5–64.5     | AX-110006357 | AX-109421639 | 16.95 | 23.81   | 0.69  | 30.8–52.0          | Chen et al. (2020), Xu et al. (2022), Zhou et al. (2017)               |
|                                |                                  | E3   | 62        | 57.5–67.5     | AX-110006357 | AX-109421639 | 16.08 | 23.60   | 1.08  | 30.8–52.0          |  |
|                                |                                  | E4   | 62        | 58.5–67.5     | AX-110006357 | AX-109421639 | 8.60  | 17.72   | 0.57  | 30.8–52.0          |  |
|                                |                                  | E2   | 18        | 17.5–18.5     | AX-110450605 | AX-110529732 | 9.44  | 3.47    | 0.47  | 138.1–148.1        |  |
|                                |                                  | E6   | 18        | 17.5–18.5     | AX-110450605 | AX-110529732 | 3.93  | 5.78    | 0.44  | 138.1–148.1        |  |
|                                |                                  | E9   | 18        | 17.5–18.5     | AX-110450605 | AX-110529732 | 5.26  | 7.22    | 0.41  | 138.1–148.1        |  |
|                                |                                  | E5   | 19        | 18.5–19.5     | AX-108899105 | AX-110418919 | 6.37  | 7.06    | 0.38  | 204.6–295.5        |  |
|                                |                                  | E8   | 19        | 18.5–19.5     | AX-108899105 | AX-110418919 | 5.28  | 10.97   | 0.39  | 204.6–295.5        |  |
|                                |                                  | E1   | 20        | 19.5–20.5     | AX-108796887 | AX-109112905 | 4.97  | 6.12    | 0.29  | 315.8–325.2        |  |
|                                |                                  | E4   | 120       | 114.5–122.5   | AX-109520051 | AX-108764357 | 3.87  | 5.95    | -0.33 | 542.4–551.2        |  |
| <i>Q<sub>Sns.ucas-5B</sub></i> | <i>Q<sub>Sns.ucas-5B</sub></i>   | E7   | 120       | 115.5–120.5   | AX-109520051 | AX-108764357 | 4.28  | 8.69    | -0.41 | 542.4–551.2        | Cui et al. (2012), Li et al. (2021a), Ma et al. (2007)                 |
|                                |                                  | E5   | 121       | 116.5–122.5   | AX-108764357 | AX-109930199 | 6.20  | 6.79    | -0.37 | 551.2–552.1        |  |
|                                |                                  | E1   | 120       | 116.5–122.5   | AX-109520051 | AX-108764357 | 4.34  | 5.63    | -0.28 | 542.4–551.2        |  |
|                                |                                  | E2   | 121       | 117.5–122.5   | AX-108764357 | AX-109930199 | 4.18  | 3.46    | -0.31 | 551.2–552.1        |  |
|                                |                                  | E2   | 56        | 49.5–57.5     | AX-110586525 | AX-110595669 | 4.18  | 11.59   | 0.50  | 18.6–30.1          |  |
|                                |                                  | E3   | 57        | 52.5–57.5     | AX-110595669 | AX-110006357 | 14.22 | 27.96   | 1.76  | 30.1–30.8          |  |
|                                |                                  | E7   | 59        | 56.5–66.5     | AX-110006357 | AX-109421639 | 6.64  | 20.69   | 1.05  | 30.8–52.0          |  |
|                                |                                  | E4   | 60        | 56.5–64.5     | AX-110006357 | AX-109421639 | 13.87 | 24.96   | 1.94  | 30.8–52.0          |  |
|                                |                                  | E6   | 61        | 57.5–67.5     | AX-110006357 | AX-109421639 | 10.76 | 18.89   | 1.18  | 30.8–52.0          |  |
|                                |                                  | E5   | 62        | 57.5–67.5     | AX-110006357 | AX-109421639 | 13.84 | 27.49   | 1.84  | 30.8–52.0          |  |
| DTH                            | <i>Q<sub>Dth.ucas-2D-1</sub></i> | E8   | 64        | 57.5–68.5     | AX-110006357 | AX-109421639 | 9.90  | 18.17   | 1.91  | 30.8–52.0          | Ma et al. (2019), Okada et al. (2019), Zhou et al. (2017); <i>ppd1</i> |

SNS spikelet number per spike, *DTH* days to heading, *Env* Environment, *Pos* position, *Chr* chromosome, *LOD* limit of detection, *PVE* phenotypic variation explained, *Add* additive effect (positive values indicate that alleles from YBM are increasing the trait scores, otherwise vice versa); the physical position is referenced with respect to the IWGSC RefSeq v2.1 coordinates  
<sup>a</sup>Known gene symbols are indicated in bold



**Fig. 2** Verification of *QSn*s. *ucas-5B* in different environments. Distribution of the polymorphic SNPs per chromosome arm (a) and the physical positions of the SNPs on chromosome 5BL according to the IWGSC RefSeq v2.1 (b). Significant differences were detected between the near-isogenic lines within the *QSn*s. *ucas-5B* region across various environments (c). The phenotypic analysis of residual heterozygous lines at the *QSn*s. *ucas-5B* locus (d). Statistical analysis was carried out using Student's *t*-test and significance was denoted by \*\* for  $P < 0.01$ . ns no significant



positions of mapped markers were relatively consistent with that in the wheat genome assembly on most of the chromosomes (Fig. S1), indicating that the genetic map constructed in the study was accurate and credible, and could be effectively used for QTL analysis.

It is worth mentioning that similar to heavily distorted distribution of markers in the 1BS/1RS region because of the linkage disequilibrium of 1RS, the markers on the short arm of chromosome 7B also showed distorted separation and were deleted during the construction of the linkage map. To examine the reasons for the distorted segregation of markers on chromosome 7B in the ZY-RILs population, we analyzed the pedigree of both parents and found that one of the ancestral parents of ZN17 is Zhoumai 11, which carries the 1BL.1RS translocation and the stripe rust resistance gene *YrZH84* (located on chromosome 7BL), both inherited from ‘Zhou8425B’, a widely used elite parent of Chinese wheat (Li 2006). Previous studies showed that all the markers (more than 40 markers) closely linked to *YrZH84* were dominant in the  $F_2$  population from the cross of Zhou8425B × ‘Chinese Spring’ (Yin et al. 2009). We hypothesized that the chromosome 7B of Zhou8425B and Chinese Spring were quite different. Moreover, an ancestral parent of Zhou8425B is ‘guangmai 74’, a hexaploid *Triticale* (AABBRR). Therefore, in combination with the results of this study, we speculated that Zhou8425B may also have an ectopic 7BL chromosome like 1BL.1RS translocation. Of course, more experiments are needed to test this surmise.

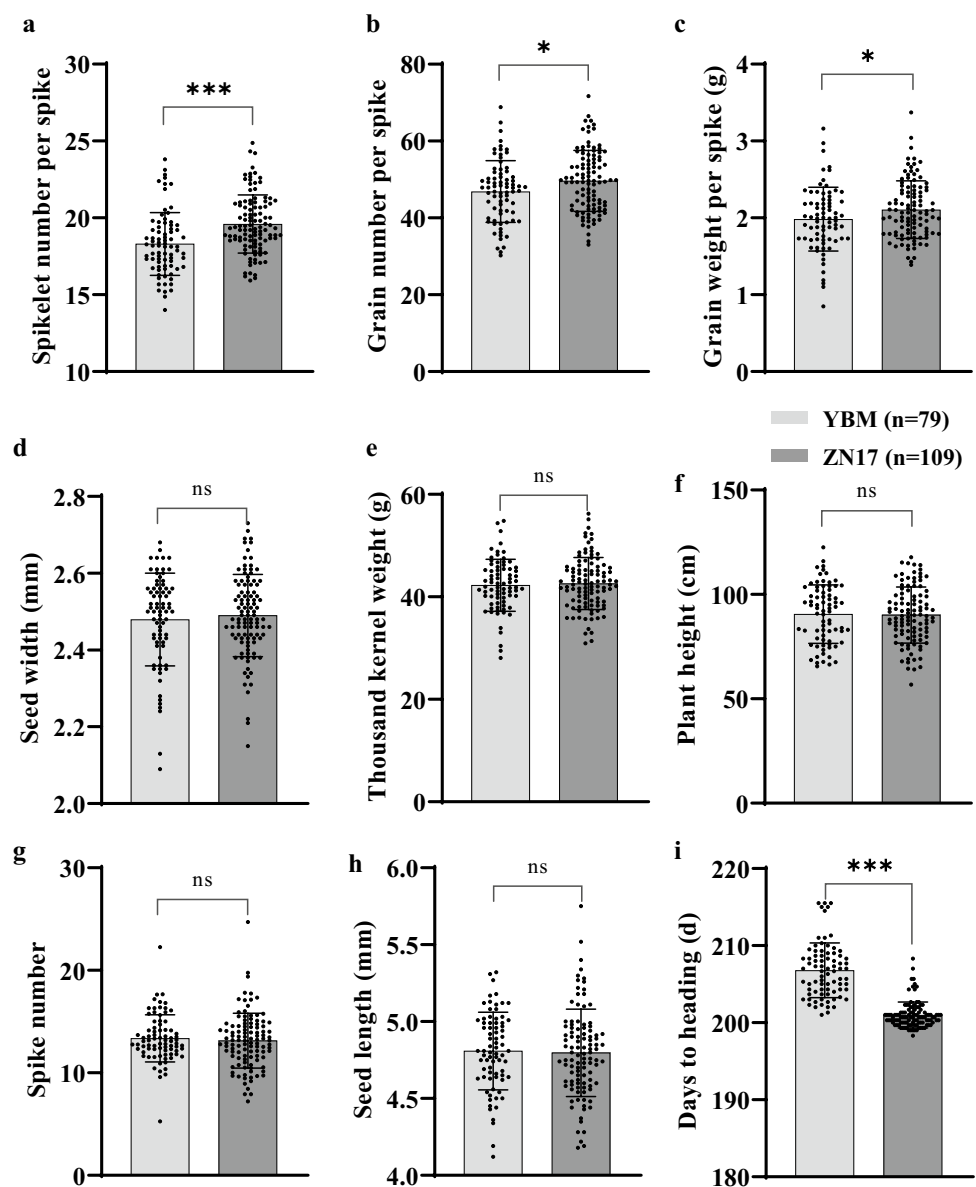
## QTL Comparison and candidate gene prediction

Like other traits related to yield, spikelet number of wheat is affected by multiple genes and significantly influenced by the environmental factors (Corsi et al. 2021). Only the stable QTL, expressing regardless of differences in environment, is convenient for marker-assisted selection strategy to improve wheat yield. In the study, we verified four stable QTLs (*QSn*s. *ucas-1B*, *QSn*s. *ucas-2D.1*, *QSn*s. *ucas-3D*, *QSn*s. *ucas-5B*) for SNS in at least five of nine different environments using this RIL population.

With reconstructed 1B full-length genetic map, the *QSn*s. *ucas-1B* was located on the 1BS chromosome and the increasing allele was derived by ZN17 (Supplementary Fig. S3). In the previous QTL studies on SNS, several mapping parents were the 1BL.1RS translocation lines, but no QTL controlling spikelet number per spike was identified in the previous studies (Cui et al. 2012; Ma et al. 2019). To the best of our knowledge, *QSn*s. *ucas-1B* is likely to be the first identified QTL controlling spikelet number per spike on 1BL.1RS translocation. However, the low genetic recombination in the 1BS/1RS translocation region complicated the mapping of interesting loci in this chromosome segment. This indicates care should be taken when genetic populations carrying alien chromosome segments are used for detecting QTL/genes of interest.

Here, *QSn*s. *ucas-2D.1* and *QDth*. *ucas-2D.1* were within an identical confidence interval (18.6–52.0 Mb) flanking

**Fig. 3** Effects of the QTL, *QSns.ucas-5B*, on various agricultural traits, including spikelet number per spike (a), grain number per spike (b), grain weight per spike (c), seed width (d), thousand kernel weight (e), plant height (f), spike number (g), seed length (h) and days to heading (i). Histograms were generated through phenotype analysis of the ZN17/YBM population that was classified into two groups based on the InDel marker. ZN17 and YBM denote the lines possessing and lacking the favorable allele of *QSns.ucas-5B*, respectively. Statistical analysis was carried out using Student's *t* test, and significance was denoted by \* and \*\*\* for  $P < 0.05$  and  $0.001$ , respectively. *ns* no significant



by markers *AX-110586525* and *AX-109421639* on chromosome 2DS, and there were 465 high-confidence genes in this region (Supplementary Table S7). *QSns/Dth.ucas-2D.1* was detected in seven environments and explained the largest phenotypic variance for SNS and DTH in the study. This QTL was located at the similar genetic region as the QTL reported by Ma et al. (2019) and Zhou et al. (2017). Notably, the region (35.1–36.7 Mb) of *QSns.sau-2D* for SNS (Ma et al. 2019) was overlapped with that of *QSns.ucas-2D.1* detected in the study. Likely to *QSns.ucas-2D.1*, *QSns.sau-2D* also had higher PVE and could be detected in all environments (Ma et al. 2019). Furthermore, Zhou et al. (2017) found that the QTL for SNS (*QTsn.cz-2D.2*), which was also related to fertile spikelet number per spike (*QFsn.cz-2D.2*) and sterile spikelet number per spike (*QSsn.cz-2D.1*). In the

flanking regions of *QSns.sau-2D*, *QTsn.cz-2D.2* and *QSns.ucas-2D.1* located a well-known gene *Ppd-D1* (36.2 Mb), which significantly affected spike length, spikelet number and heading date in wheat (Okada et al. 2019). We analyzed the allele types of *Ppd-D1* between the two parents according to the method described by Beales et al. (2007) and found that ZN17 belonged to *Ppd-D1a* allele, while YBM belonged to *Ppd-D1b* type. In light of the fact that *QSns.ucas-2D.1* and *QDth.ucas-2D.1* were located within an overlapping confidence interval, we put forth the hypothesis that *Ppd-D1* is the most favorable candidate gene for *QSns/Dth.ucas-2D.1*.

*QSns.ucas-3D*, detected in six environments, was mapped to an interval flanked by markers *AX-110450605* and *AX-109112905* and physically located between 138.1 and

325.2 Mb spanning 187.1 Mb on chromosome 3D. To the best of our knowledge, a few QTLs for spike-related traits were found on 3D chromosome. Li et al. (2021a) reported a novel QTL *QTsn/Fsn.cib-3D* associated with both SNS and fertile spikelet number per spike located in a 4.5-cM interval on chromosome arm 3DL flanked by *AX-109429351* (550.3 Mb) and *AX-110914105* (555.1 Mb). *QSspn.cau-3D* (Chen et al. 2020) and *QSsn.cau-3D* (Zhou et al. 2017) for sterile spikelet number in total were located in nearly the same genomic region (~87.6–96.5 Mb) on 3DS. *QSc.cau-3D.1* with a LOD score of 6.65 explained 11.12% of spike compactness variation, sharing identical confidence interval with *QSl.cau-3D* for spike length (~30.4–60.0 Mb) reported by Xu et al. (2022). Thus, *QSns.ucas-3D* identified in the study appeared to be a novel locus located in the downstream of *QSspn.cau-3D* and *QSsn.cau-3D*, and the upstream of *QTsn/Fsn.cib-3D*, respectively. A total of 1996 high-confidence genes were identified within the intervals of *QSns.ucas-3D*. However, due to the relatively high number of genes in this region, the prediction of candidate genes appears to be a daunting task, rendering additional studies necessary for the fine mapping of the QTL.

In this study, we validated the *QSns.ucas-5B* locus using a RHL approach and mapped it to the genomic interval ranging from 545.4 to 552.1 Mb on the long arm of chromosome 5B. Ma et al. (2007) have mapped a QTL, *QSpn.nau-5B*, for SNS to an interval (480.5–507.3 Mb, flanked by markers *Xgwm499* and *Xgwm639*) close to that of *QSns.ucas-5B*. Subsequently, Cui et al. (2012) found that *QSpn.WJ.5B.2* confirmed the QTL for SNS detected by Ma et al. (2007). Additionally, Li et al. (2021a) identified the *QTsn/Fsn.cib-5B* locus controlling both total spike number and fertile spike number at the physical position of 568.3–569.2 Mb on chromosome 5B, flanked by the markers *AX-108863479* and *AX-109820694*. Given the proximity of the physical location of *QTsn/Fsn.cib-5B* and the *QSns.ucas-5B* locus identified in our study, we analyzed SNP markers surrounding the peak of *QTsn/Fsn.cib-5B* and found its genetic distance in our constructed linkage map to be approximately 280.2–283.8 cM (Supplementary Table S10), which significantly differed from the peak at 252.5–262.5 cM detected in our study. Furthermore, through analysis of the remaining heterozygous lines at the *QSns.ucas-5B* locus using a 660 K wheat chip, we found no overlap interval with the mapping region detected by Li et al. (2021a), with the heterozygous interval located at 545–560 Mb. Comparison of physical position of reported QTL for SNS indicated that *QSns.ucas-5B* identified in the study may be a new locus. To validate the effect of *QSns.ucas-5B*, we evaluated the phenotypes with the near-isogenic lines at *QSns.ucas-5B* locus in the field. The results showed that the elite haplotype from ZN17 than that from YBM significantly increased SNS, ranging

from 1.31 (6.74%) to 2.54 (13.17%), at multiple environments (Fig. 2c). Moreover, we found that this locus had no influence on PH, SN and seed shape, but moderate positive influence on GNS and GWS (Fig. 3a–h). Importantly, we also discovered that the allele of ZN17 can significantly increase spikelet number and spikelet weight without delaying the heading stage (Fig. 3), indicating the potential of *QSns.ucas-5B* as a promising locus for maturity and yield breeding. The early flowering and higher spikelet number associated with the ZN17 allele at *QSns.ucas-5B* locus is particularly interesting. Regarding the co-occurrence of these opposing traits in ZN17, we guess although ZN17 exhibits an earlier heading, it is possible that the sub-phase durations of spike development are extended. Additionally, considering that ZN17 is a cultivated variety while YBM is a landrace, we speculate that ZN17 may have significantly higher photosynthetic efficiency or nitrogen utilization efficiency compared to YBM. This may contribute ZN17 to accumulate more nutrients in a shorter timeframe, facilitating floral bud differentiation and the formation of spikes.

In this study, we have successfully constructed a high-density genetic map for a ZY-RILs population containing 95,444 SNPs spanning a total distance of 4232.42 cM. Using multiple environmental conditions, a total of 15 QTLs for SNS and 6 QTLs for DTH were identified. Remarkably, four stable QTLs for SNS were discovered across more than five environmental conditions, demonstrating a PVE ranging from 1.90 to 23.81%. Among them, *QSns.ucas-1B* was found to be located in the 1RS/1BS region, while *QSns.ucas-2D.1* and *QDth.ucas-2D.1* were found to be co-localized and associated with *Ppd1*. *QSns.ucas-3D* was identified as a novel QTL for SNS. We also confirmed the existence of a promising SNS locus, *QSns.ucas-5B*, which was found to be associated with GNS and GWS, while not delaying the heading. A linkage marker *InDel-SNS5B* was developed for marker-assisted selection. Overall, this research provides a deeper understanding of the genetic foundation of SNS and is expected to facilitate the improvement for SNS and cloning of genes associated with *QSns.ucas-5B* in future studies.

**Supplementary Information** The online version contains supplementary material available at <https://doi.org/10.1007/s00122-023-04488-7>.

**Authors' Contributions** H-Q L and SZ conceived the project and revised the manuscript; SZ developed the mapping population; YS, ST, JN, ZY, SM, QL and HW carried out the experiments; YS analyzed data and wrote the manuscript; all authors assisted in revising the manuscript.

**Funding** This work was supported by grants from the Strategic Priority Research Program of Chinese Academy of Sciences (Grant No. XDA24010104-1) and China Postdoctoral Science Foundation (2022M710163).

**Availability of data and material** All data generated or analyzed during this study are included in the main text article and its supplementary files. The raw sequencing data of ZN17 and YBM have been deposited in National Genomics Data Center (NGDC, <https://ngdc.cnecb.ac.cn/>) under accession numbers CRR290233 and CRR290167, respectively.

## Declarations

**Conflict of interest** The authors declare that they have no conflicts of interest.

**Code availability** Not applicable.

**Consent to participate** Not applicable.

**Consent for publication** Not applicable.

**Ethics approval** Not applicable.

## References

- Beales J, Turner A, Griffiths S, Snape JW, Laurie DA (2007) A *Pseudo-Response Regulator* is misexpressed in the photoperiod insensitive *Ppd-D1a* mutant of wheat (*Triticum aestivum* L.). *Theor Appl Genet* 115:721–733
- Boden SA, Cavanagh C, Cullis BR, Ramm K, Greenwood J, Jean Finnegan E, Trevaskis B, Swain SM (2015) *Ppd-1* is a key regulator of inflorescence architecture and paired spikelet development in wheat. *Nat Plants* 1:14016
- Chen Z, Ke W, He F, Chai L, Cheng X, Xu H, Wang X, Du D, Zhao Y, Chen X, Xing J, Xin M, Guo W, Hu Z, Su Z, Liu J, Peng H, Yao Y, Sun Q, Ni Z (2022) A single nucleotide deletion in the third exon of *FT-D1* increases the spikelet number and delays heading date in wheat (*Triticum aestivum* L.). *Plant Biotechnol J* 20:920–933
- Chen ZY, Cheng XJ, Chai LL, Wang ZH, Du DJ, Wang ZH, Bian RL, Zhao AJ, Xin MM, Guo WL, Hu ZR, Peng HR, Yao YY, Sun QX, Ni ZF (2020) Pleiotropic QTL influencing spikelet number and heading date in common wheat (*Triticum aestivum* L.). *Theor Appl Genet* 133:1825–1838
- Chhetri M, Bariana H, Wong D, Sohail Y, Hayden M, Bansal U (2017) Development of robust molecular markers for marker-assisted selection of leaf rust resistance gene *Lr23* in common and durum wheat breeding programs. *Mol Breed* 37:21
- Corsi B, Obinu L, Zanella CM, Cutrupi S, Day R, Geyer M, Lillemo M, Lin M, Mazza L, Percival-Alwyn L, Stadlmeier M, Mohler V, Hartl L, Cockram J (2021) Identification of eight QTL controlling multiple yield components in a German multi-parental wheat population, including *Rht24*, *WAPO-A1*, *WAPO-B1* and genetic loci on chromosomes 5A and 6A. *Theor Appl Genet* 134:1435–1454
- Cui F, Ding A, Li J, Zhao C, Wang L, Wang X, Qi X, Li X, Li G, Gao J, Wang H (2012) QTL detection of seven spike-related traits and their genetic correlations in wheat using two related RIL populations. *Euphytica* 186:177–192
- Cui F, Zhang N, Fan X-l, Zhang W, Zhao C-h, Yang L-j, Pan R-q, Chen M, Han J, Zhao X-q, Ji J, Tong Y-p, Zhang H-x, Jia J-z, Zhao G-y, Li J-m (2017) Utilization of a Wheat660K SNP array-derived high-density genetic map for high-resolution mapping of a major QTL for kernel number. *Sci Rep* 7:3788
- Dixon LE, Greenwood JR, Bencivenga S, Zhang P, Cockram J, Mellers G, Ramm K, Cavanagh C, Swain SM, Boden SA (2018) *TEOSINTE BRANCHED1* regulates inflorescence architecture and development in bread wheat (*Triticum aestivum*). *Plant Cell* 30:563–581
- Dobrovolskaya O, Pont C, Sibout R, Martinek P, Badaeva E, Murat F, Chosson A, Watanabe N, Prat E, Gautier N, Gautier V, Poncet C, Orlov YL, Krasnikov AA, Bergès H, Salina E, Laikova L, Salse J (2015) *FRIZZY PANICLE* drives supernumerary spikelets in bread wheat. *Plant Physiol* 167:189–199
- Echeverry-Solarte M, Kumar A, Kianian S, Simsek S, Alamri MS, Mantovani EE, McClean PE, Deckard EL, Elias E, Schatz B (2015) New QTL alleles for quality-related traits in spring wheat revealed by RIL population derived from supernumerary×non-supernumerary spikelet genotypes. *Theor Appl Genet* 128:893–912
- He GH, Zhang YW, Liu P, Jing YX, Zhang LC, Zhu YF, Kong XY, Zhao HX, Zhou Y, Sun JQ (2021) The transcription factor TaLAX1 interacts with Q to antagonistically regulate grain threshability and spike morphogenesis in bread wheat. *New Phytol* 230:988–1002
- Holland J, Nyquist W, Cervantes-Martinez C (2003) Estimating and interpreting heritability for plant breeding. *Plant Breed Rev* 22:9–111
- Huang X, Qian Q, Liu Z, Sun H, He S, Luo D, Xia G, Chu C, Li J, Fu X (2009) Natural variation at the *DEP1* locus enhances grain yield in rice. *Nat Genet* 41:494–497
- Isham K, Wang R, Zhao W, Wheeler J, Klassen N, Akhunov E, Chen J (2021) QTL mapping for grain yield and three yield components in a population derived from two high-yielding spring wheat cultivars. *Theor Appl Genet* 134:2079–2095
- Kitomi Y, Ogawa A, Kitano H, Inukai Y (2008) *CRL4* regulates crown root formation through auxin transport in rice. *Plant Root* 2:19–28
- Kuzay S, Lin H, Li C, Chen S, Woods DP, Zhang J, Lan T, von Korff M, Dubcovsky J (2022) *WAPO-A1* is the causal gene of the 7AL QTL for spikelet number per spike in wheat. *PLoS Genet* 18:e1009747–e1009747
- Lewis JM, Mackintosh CA, Shin S, Gilding E, Kravchenko S, Baldrige G, Zeyen R, Muehlbauer GJ (2008) Overexpression of the maize *Teosinte Branched1* gene in wheat suppresses tiller development. *Plant Cell Rep* 27:1217–1225
- Li T, Deng G, Tang Y, Su Y, Wang J, Cheng J, Yang Z, Qiu X, Pu X, Zhang H, Liang J, Yu M, Wei Y, Long H (2021a) Identification and validation of a novel locus controlling spikelet number in bread wheat (*Triticum aestivum* L.). *Front Plant Sci* 12:611106
- Li Y, Li L, Zhao M, Guo L, Guo X, Zhao D, Batool A, Dong B, Xu H, Cui S, Zhang A, Fu X, Li J, Jing R, Liu X (2021b) Wheat *FRIZZY PANICLE* activates *VERNALIZATION1-A* and *HOMEBOX4-A* to regulate spike development in wheat. *Plant Biotechnol J* 19:1141–1154
- Li ZF (2006) Identification of slow stripe rust resistance in Chinese wheat and molecular mapping of new stripe rust resistance gene *YrZH84*. Ph.D. Thesis. Chinese academy of agricultural sciences
- Liu H, Wang K, Tang H, Gong Q, Du L, Pei X, Ye X (2020) CRISPR/Cas9 editing of wheat *TaQ* genes alters spike morphogenesis and grain threshability. *J Genet Genom* 47:563–575
- Liu J, Luo W, Qin N, Ding P, Zhang H, Yang C, Mu Y, Tang H, Liu Y, Li W, Jiang Q, Chen G, Wei Y, Zheng Y, Liu C, Lan X, Ma J (2018) A 55 K SNP array-based genetic map and its utilization in QTL mapping for productive tiller number in common wheat. *Theor Appl Genet* 131:2439–2450
- Ma J, Ding P, Liu J, Li T, Zou Y, Habib A, Mu Y, Tang H, Jiang Q, Liu Y (2019) Identification and validation of a major and stably expressed QTL for spikelet number per spike in bread wheat. *Theor Appl Genet* 132:3155–3167
- Ma S, Wang M, Wu J, Guo W, Chen Y, Li G, Wang Y, Shi W, Xia G, Fu D, Kang Z, Ni F (2021) WheatOmics: a platform combining multiple omics data to accelerate functional genomics studies in wheat. *Mol Plant* 14:1965–1968

- Ma Z, Zhao D, Zhang C, Zhang Z, Xue S, Lin F, Kong Z, Tian D, Luo Q (2007) Molecular genetic analysis of five spike-related traits in wheat using RIL and immortalized F<sub>2</sub> populations. *Mol Genet Genom* 277:31–42
- Mcintosh RA, Dubcovsky J, Rogers WJ, Morris C, Appels R, Xia XC (2017) Catalogue of gene symbols for wheat: 2017 Supplement
- Meng L, Li HH, Zhang LY, Wang JK (2015) QTL IciMapping: Integrated software for genetic linkage map construction and quantitative trait locus mapping in biparental populations. *Crop J* 3:269–283
- Muqaddasi QH, Brassac J, Koppolu R, Plieske J, Ganai MW, Röder MS (2019) *TaAPO-A1*, an ortholog of rice *ABERRANT PANICLE ORGANIZATION 1*, is associated with total spikelet number per spike in elite European hexaploid winter wheat (*Triticum aestivum* L.) varieties. *Sci Rep* 9:13853
- Okada T, Jayasinghe JEARM, Eckermann P, Watson-Haigh NS, Warner P, Hendrikse Y, Baes M, Tucker EJ, Laga H, Kato K, Albertsen M, Wolters P, Fleury D, Baumann U, Whitford R (2019) Effects of *Rht-B1* and *Ppd-D1* loci on pollinator traits in wheat. *Theor Appl Genet* 132:1965–1979
- Peng L-T, Shi Z-Y, Li L, Shen G-Z, Zhang J-L (2007) Ectopic expression of *OsLFL1* in rice represses *Ehd1* by binding on its promoter. *Biochem Bioph Res Co* 360:251–256
- Quarrie SA, Quarrie SP, Radošević R, Rancic D, Kaminska A, Barnes JD, Leverington M, Ceoloni C, Dodig D (2006) Dissecting a wheat QTL for yield present in a range of environments: from the QTL to candidate genes. *J Exp Bot* 57:2627–2637
- Ronin YI, Mester DI, Minkov DG, Akhunov E, Korol AB (2017) Building ultra-high-density linkage maps based on efficient filtering of trustable markers. *Genetics* 206:1285–1295
- Shaw LM, Bo L, Turner R, Li C, Dubcovsky J (2018) *FLOWERING LOCUS T2 (FT2)* regulates spike development and fertility in temperate cereals. *J Exp Bot* 70:193–204
- Si Y, Zheng S, Niu J, Tian S, Shi X, He Y, Li Y, Ling H-Q (2021) Fine mapping of hybrid necrosis gene *Ne1* in common wheat (*Triticum aestivum* L.). *Theor Appl Genet* 134:2603–2611
- Si Y, Lu Q, Tian S, Niu J, Cui M, Liu X, Gao Q, Shi X, Ling H-Q, Zheng S (2022) Fine mapping of the tiller inhibition gene *TIN5* in *Triticum urartu*. *Theor Appl Genet* 135:2665–2673
- Simmonds J, Scott P, Brinton J, Mestre TC, Bush M, del Blanco A, Dubcovsky J, Uauy C (2016) A splice acceptor site mutation in *TaGW2-A1* increases thousand grain weight in tetraploid and hexaploid wheat through wider and longer grains. *Theor Appl Genet* 129:1099–1112
- Simons KJ, Fellers JP, Trick HN, Zhang ZC, Tai YS, Gill BS, Faris JD (2006) Molecular characterization of the major wheat domestication gene *Q*. *Genetics* 172:547–555
- Song G, Sun G, Kong X, Jia M, Wan K, Ye X, Zhou Y, Geng S, Mao L, Li A (2019) The soft glumes of common wheat are sterile-lemmas as dete fined by the domestication gene *Q*. *Crop J* 7:113–117
- Song S, Wang G, Hu Y, Liu H, Bai X, Qin R, Xing Y (2018) *OsMFT1* increases spikelets per panicle and delays heading date in rice by suppressing *Ehd1*, *FZP* and *SEPALLATA*-like genes. *J Exp Bot* 69:4283–4293
- Sreenivasulu N, Schnurbusch T (2012) A genetic playground for enhancing grain number in cereals. *Trends Plant Sci* 17:91–101
- Sun C, Dong Z, Zhao L, Ren Y, Zhang N, Chen F (2020) The Wheat 660K SNP array demonstrates great potential for marker-assisted selection in polyploid wheat. *Plant Biotechnol J* 18:1354–1360
- Sun C, Zhang F, Yan X, Zhang X, Dong Z, Cui D, Chen F (2017) Genome-wide association study for 13 agronomic traits reveals distribution of superior alleles in bread wheat from the Yellow and Huai Valley of China. *Plant Biotechnol J* 15:953–969
- Wang YG, Du F, Wang J, Wang K, Tian CH, Qi XQ, Lu F, Liu XG, Ye XG, Jiao YL (2022) Improving bread wheat yield through modulating an unselected AP2/ERF gene. *Nat Plants* 8:930–939
- Wurschum T, Leiser WL, Langer SM, Tucker MR, Longin CFH (2018) Phenotypic and genetic analysis of spike and kernel characteristics in wheat reveals long-term genetic trends of grain yield components. *Theor Appl Genet* 131:2071–2084
- Xu H, Zhang R, Wang M, Li L, Yan L, Wang Z, Zhu J, Chen X, Zhao A, Su Z, Xing J, Sun Q, Ni Z (2022) Identification and characterization of QTL for spike morphological traits, plant height and heading date derived from the D genome of natural and resynthetic allohexaploid wheat. *Theor Appl Genet* 135:389–403
- Yao H, Xie Q, Xue S, Luo J, Lu J, Kong Z, Wang Y, Zhai W, Lu N, Wei R, Yang Y, Han Y, Zhang Y, Jia H, Ma Z (2019) HL2 on chromosome 7D of wheat (*Triticum aestivum* L.) regulates both head length and spikelet number. *Theor Appl Genet* 132:1789–1797
- Yin G, Wang J, Wen W, He Z, Li Z, Wang H, Xia X (2009) Mapping of wheat stripe rust resistance gene *YrZH84* with RGAP markers and its application. *Acta Agron Sin* 35:1274–1281
- Zhai H, Feng Z, Du X, Song Y, Liu X, Qi Z, Song L, Li J, Li L, Peng H, Hu Z, Yao Y, Xin M, Xiao S, Sun Q, Ni Z (2018) A novel allele of *TaGW2-A1* is located in a finely mapped QTL that increases grain weight but decreases grain number in wheat (*Triticum aestivum* L.). *Theor Appl Genet* 131:539–553
- Zhang B, Liu X, Xu W, Chang J, Li A, Mao X, Zhang X, Jing R (2015) Novel function of a putative *MOCl* ortholog associated with spikelet number per spike in common wheat. *Sci Rep* 5:12211
- Zhang XY, Jia HY, Li T, Wu JZ, Nagarajan R, Lei L, Powers C, Kan CC, Hua W, Liu ZY, Chen C, Carver BF, Yan LL (2022) *TaCol-B5* modifies spike architecture and enhances grain yield in wheat. *Science* 376:180–183
- Zhao K, Xiao J, Liu Y, Chen S, Yuan C, Cao A, You FM, Yang D, An S, Wang H, Wang X (2018) *Rht23 (5Dq)* likely encodes a *Q* homeologue with pleiotropic effects on plant height and spike compactness. *Theor Appl Genet* 131:1825–1834
- Zhou Y, Conway B, Miller D, Marshall D, Cooper A, Murphy P, Chao S, Brown-Guedira G, Costa J (2017) Quantitative trait loci mapping for spike characteristics in hexaploid wheat. *Plant Genome* 10:2
- Zhu TT, Wang L, Rimbart H, Rodriguez JC, Deal KR, De Oliveira R, Choulet F, Keeble-Gagnere G, Tibbits J, Rogers J, Eversole K, Appels R, Gu YQ, Mascher M, Dvorak J, Luo MC (2021) Optical maps refine the bread wheat *Triticum aestivum* cv. Chinese Spring genome assembly. *Plant J* 107:303–314

**Publisher's Note** Springer Nature remains neutral with regard to jurisdictional claims in published maps and institutional affiliations.

Springer Nature or its licensor (e.g. a society or other partner) holds exclusive rights to this article under a publishing agreement with the author(s) or other rightsholder(s); author self-archiving of the accepted manuscript version of this article is solely governed by the terms of such publishing agreement and applicable law.